

Living Ziegler–Natta Polymerization by Early Transition Metals: Synthesis and Evaluation of Cationic Zirconium Alkyl Complexes Bearing β -Hydrogens as Models for Propagating Centers

Matthew B. Harney, Richard J. Keaton, James C. Fettinger, and Lawrence R. Sita*

Contribution from the Department of Chemistry and Biochemistry, University of Maryland, College Park, Maryland 20742

Received November 19, 2005; E-mail: lsita@umd.edu

Abstract: The synthesis and characterization of a series of cationic zirconium and hafnium complexes with alkyl substituents bearing β -hydrogens of general formula $\{(\eta^5\text{-C}_5\text{Me}_5)\text{MR}[\text{N}(\text{Et})\text{C}(\text{Me})\text{N}(\text{t-Bu})]\}[\text{B}(\text{C}_6\text{F}_5)_4]$ [$\text{M} = \text{Zr}$; $\text{R} = \text{Et}$, $n\text{-Pr}$, $i\text{-Pr}$, $n\text{-Bu}$, $i\text{-Bu}$, and 2-ethylbutyl (**5a–f**) and $\text{M} = \text{Hf}$; $\text{R} = i\text{-Bu}$ and $t\text{-Bu}$ (**6** and **7**, respectively)] is described, including several isotopically labeled derivatives. The ability of these complexes to serve as model complexes for the living Ziegler–Natta polymerization of olefins that can be effected using the initiator **2a** ($\text{R} = \text{Me}$ in **5**) has been addressed. The results obtained shed additional light on the steric and electronic factors that can contribute to the living character of a Ziegler–Natta polymerization based on an early transition metal initiator.

Introduction

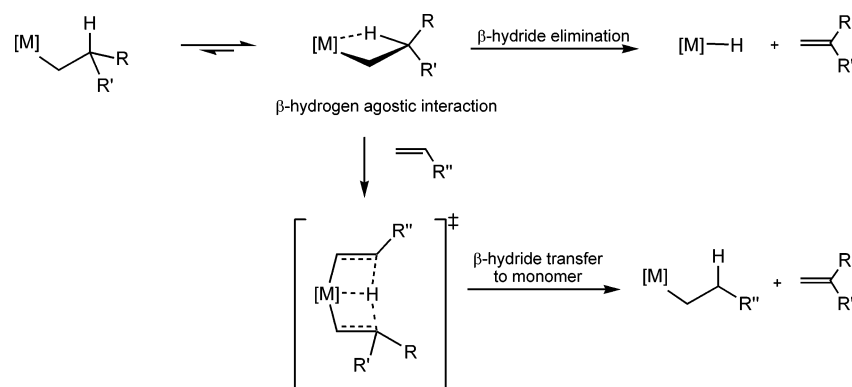
The development of well-defined transition metal complexes that can serve as initiators for the living, and in some cases stereospecific, polymerization of α -olefins is the latest chapter in a decades-long success story that has covered the discovery, mechanistic understanding, and commercialization of homogeneous “single-site” catalysts for polyolefin production through the Ziegler–Natta process.^{1–11} However, in contrast to the wealth of experimental and theoretical information now available regarding the various mechanisms for chain termination and chain release in *nonliving* group 4 bis(cyclopentadienyl)metal-based systems (also known as metallocenes), which are largely dominated by mononuclear β -hydride elimination and β -hydride transfer reactions,¹² little is still known of the structural and

electronic factors that are required to allow a propagating center involving an early transition metal to continue to propagate without such type of termination. Once this knowledge becomes available, though, the design of second and third generation initiators for (stereospecific) living Ziegler–Natta polymerizations that can operate at higher temperatures, and for a wider range of monomers, should be feasible.

For group 4 metallocenes, cationic complexes bearing alkyl groups with β -hydrogens, and typically either an ethyl or isobutyl group, have long been considered as viable experimental and theoretical models for the proposed polymer chain-bound propagating center.^{12,13} Further, from these studies, it is now widely accepted that observation of a strong intramolecular

- (1) For a review of living Ziegler–Natta polymerization, see: Coates, G. W.; Hustad, P. D.; Reinartz, S. *Angew. Chem., Int. Ed.* **2002**, *41*, 2236–2257.
- (2) For recent reviews of homogeneous Ziegler–Natta polymerization, see: (a) Brintzinger, H. H.; Fischer, D.; Mülhaupt, R.; Rieger, B.; Waymouth, R. M. *Angew. Chem., Int. Ed. Engl.* **1995**, *34*, 1143–1170. (b) Coates, G. W. *Chem. Rev.* **2000**, *100*, 1223–1252. (c) Gibson, V. C.; Spitzmesser, S. K. *Chem. Rev.* **2003**, *103*, 283–315.
- (3) (a) Scollard, J. D.; McConville, D. H. *J. Am. Chem. Soc.* **1996**, *118*, 10008–10009. (b) Scollard, J. D.; McConville, D. H.; Rettig, S. J. *Organometallics* **1997**, *16*, 1810–1812. (c) Scollard, J. D.; McConville, D. H.; Vittal, J. J.; Payne, N. C. *J. Mol. Catal. A* **1998**, *128*, 201–204.
- (4) (a) Baumann, R.; Davis, W. M.; Schrock, R. R. *J. Am. Chem. Soc.* **1997**, *119*, 3830–3831. (b) Baumann, R.; Schrock, R. R. *J. Organomet. Chem.* **1998**, *557*, 69–75. (c) Schrock, R. R.; Baumann, R.; Reid, S. M.; Goodman, J. T.; Stumpf, R.; Davis, W. M. *Organometallics* **1999**, *18*, 3649–3670. (d) Mehrkhodavandi, P.; Bonitatebus, P. J.; Schrock, R. R. *J. Am. Chem. Soc.* **2000**, *122*, 7841–7842. (e) Mehrkhodavandi, P.; Schrock, R. R. *J. Am. Chem. Soc.* **2001**, *123*, 10746–10747. (f) Mehrkhodavandi, P.; Schrock, R. R.; Bonitatebus, P. J., Jr. *Organometallics* **2002**, *21*, 5785–5798. (g) Mehrkhodavandi, P.; Schrock, R. R.; Pryor, L. L. *Organometallics* **2003**, *22*, 4569–4583. (h) Schrock, R. R.; Adamchuk, J.; Ruhland, K.; Lopez, L. P. H. *Organometallics* **2005**, *24*, 857–866.
- (5) (a) Hagihara, H.; Shiono, T.; Ikeda, T. *Macromolecules* **1998**, *31*, 3184–3188. (b) Hasan, T.; Ioku, A.; Nishii, K.; Shiono, T.; Ikeda, T. *Macromolecules* **2001**, *34*, 3142–3146. (c) Nishii, K.; Shiono, T.; Ikeda, T. *Macromol. Rapid Commun.* **2004**, *25*, 1029–1032.
- (6) (a) Jayaratne, K. C.; Sita, L. R. *J. Am. Chem. Soc.* **2000**, *122*, 958–959. (b) Jayaratne, K. C.; Keaton, R. J.; Henningsen, D. A.; Sita, L. R. *J. Am. Chem. Soc.* **2000**, *122*, 10490–10491. (c) Keaton, R. J.; Jayaratne, K. C.; Fettinger, J. C.; Sita, L. R. *J. Am. Chem. Soc.* **2000**, *122*, 12909–12910. (d) Keaton, R. J.; Jayaratne, K. C.; Henningsen, D. A.; Koterwas, L. A.; Sita, L. R. *J. Am. Chem. Soc.* **2001**, *123*, 6197–6198. (e) Jayaratne, K. C.; Sita, L. R. *J. Am. Chem. Soc.* **2001**, *123*, 10754–10755. (f) Zhang, Y.; Keaton, R. J.; Sita, L. R. *J. Am. Chem. Soc.* **2003**, *125*, 9062–9069. (g) Zhang, Y.; Sita, L. R. *J. Am. Chem. Soc.* **2004**, *126*, 7776–7777. (h) Kissounko, D. A.; Zhang, Y.; Harney, M. B.; Sita, L. R. *Adv. Synth. Catal.* **2005**, *347*, 426–432.
- (7) (a) Tshuva, E. Y.; Goldberg, I.; Kol, M. *J. Am. Chem. Soc.* **2000**, *122*, 10706–10707. (b) Tshuva, E. Y.; Goldberg, I.; Kol, M.; Goldschmidt, Z. *J. Chem. Soc., Chem. Commun.* **2001**, 2120–2121. (c) Segal, S.; Goldberg, I.; Kol, M. *Organometallics* **2005**, *24*, 200–202.
- (8) (a) Mitani, M.; Mohri, J.-I.; Yoshida, Y.; Saito, J.; Ishii, S.; Tsuru, K.; Matsui, S.; Furuyama, R.; Nakano, T.; Tanaka, H.; Kojoh, S.-I.; Matsugi, T.; Kashiwa, N.; Fujita, T. *J. Am. Chem. Soc.* **2002**, *124*, 3327–3336. (b) Mitani, M.; Nakano, T.; Fujita, T. *Chem. Eur. J.* **2003**, *9*, 2396–2403. (c) Suzuki, Y.; Terao, H.; Fujita, T. *Bull. Chem. Soc. Jpn.* **2003**, *76*, 1493–1517. (d) Makio, H.; Fujita, T. *Bull. Chem. Soc. Jpn.* **2005**, *78*, 52–66.
- (9) (a) Tian, J.; Coates, G. W. *Angew. Chem., Int. Ed.* **2000**, *39*, 3626–3629. (b) Tian, J.; Hustad, P. D.; Coates, G. W. *J. Am. Chem. Soc.* **2001**, *123*, 5134–5135. (c) Mason, A. F.; Coates, G. W. *J. Am. Chem. Soc.* **2004**, *126*, 16326–16327.
- (10) (a) Busico, V.; Cipullo, R.; Friederichs, N.; Ronca, S.; Togrou, M. *Macromolecules* **2003**, *36*, 3806–3808. (b) Busico, V.; Cipullo, R.; Friederichs, N.; Ronca, S.; Talarico, G.; Togrou, M.; Wang, B. *Macromolecules* **2004**, *37*, 8201–8203.

Scheme 1



agostic interaction between the metal center and a hydrogen atom in the β -position of an alkyl substituent is a strong predictor for β -hydride elimination, or β -hydride transfer, according to Scheme 1.¹⁴ Given this, it is reasonable to expect that, by preventing the formation of β -hydrogen agostic interactions, perhaps through steric control of the ligand environment about the metal center, one should be able to design systems that are living by shutting down these termination pathways, assuming, of course, that no other termination pathways exist. Indeed, Schrock and co-workers⁴ have presented such a steric argument to rationalize the living character of polymerizations mediated by their $\{[\text{NON}]\text{ZrMe}\}^+[\text{B}(\text{C}_6\text{F}_5)_4]^-$ ($[\text{NON}]^{2-} = [\text{t-Bu-d}_6\text{-N-}o\text{-C}_6\text{H}_4\text{O}]^{2-}$) initiator, where β -hydride elimination involving the polymer chain is seen to occur only very slowly at 0 °C. Further, in another of their living systems, direct observation by ¹H NMR spectroscopy of the cationic isobutyl initiators, $\{[\text{MesNpy}]\text{M}(\text{i-Bu})\}^+[\text{B}(\text{C}_6\text{F}_5)_4]^-$ ($\text{M} = \text{Zr}$ and Hf ; $[\text{MesNpy}]^{2-} = [\text{H}_3\text{CC}(2\text{-C}_5\text{H}_4\text{N})(\text{CH}_2\text{Nmesityl})_2]^{2-}$), did not reveal any evidence for a β -hydrogen agostic interaction between the metal and the methine proton of the isobutyl group. In apparent accordance, then, with expectations based on the absence of such a β -hydrogen agostic interaction, both of these initiators for $\text{M} = \text{Zr}$ and Hf were found to decompose only very slowly at 0 °C in a strictly first-order fashion via assumed β -hydride elimination, with $t_{1/2} = 40$ min for $\text{M} = \text{Zr}$ and $t_{1/2} = 21$ h for $\text{M} = \text{Hf}$.^{4g}

Fujita and co-workers⁸ have recently presented a different hypothesis to account for the surprising robustness of their titanium bis(phenoxyimine)-based system, derived from activation of $\text{TiCl}_2\{\eta^2\text{-1-[C(H)=N(C}_6\text{F}_5)_2\text{-O-3-(t-Bu)C}_6\text{H}_3\text{]}_2\}$ with methylaluminoxane (MAO), that is capable of effecting the

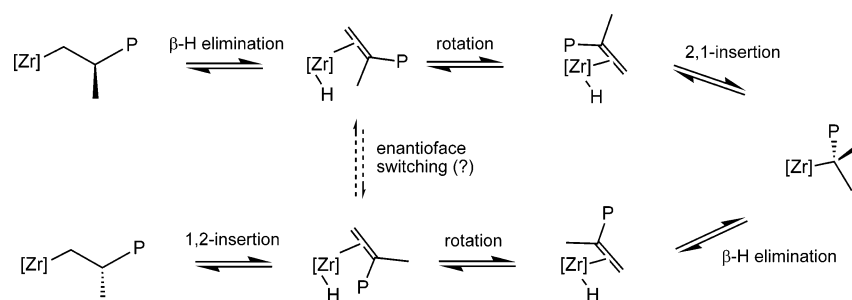
living polymerization of ethene and propene at 50 °C. On the basis of DFT calculations, these investigators attributed the observed remarkable stability of the propagating center to an attractive force between an *ortho*-fluorine of the *N*-pentafluorophenyl group within the ligand and a β -hydrogen on the growing polymer chain that they feel is strong enough to mitigate formation of a β -hydrogen agostic interaction with the metal center, thereby preventing both β -hydride elimination and β -hydride transfer to monomer. Chan and co-workers¹⁵ have recently provided solution NMR evidence for a $\text{H}\cdots\text{F}$ interaction between a fluorine atom of an *ortho*-CF₃ phenyl substituent and the α -hydrogen of a benzyl group within a neutral (phenoxy-pyridine)zirconium benzyl complex, and they have proposed that, while not being a direct model, this observation lends support to the Fujita hypothesis. However, subsequent theoretical investigations indicate that the effects of the *ortho*-fluorine atoms in the Fujita system are, at best, primarily *steric* in nature and serve to destabilize the transition state for β -hydride transfer to monomer.¹⁶

In addition to termination, β -hydride elimination within a propagating center appears to be capable of playing a critical role in introducing stereoerrors within the polymer microstructure when propene is polymerized by group 4 metallocene-based catalysts under conditions of low monomer concentration.^{17–20} As Scheme 2 reveals, these stereoerrors appear to be the result of an overall “chain-end epimerization” process that proceeds through two consecutive sequences of steps involving β -hydride elimination, alkene rotation about the metal, and reinsertion. Originally proposed by Busico and co-workers,¹⁷ this mechanism has received considerable support through polymerization studies involving isotopically labeled propene by groups of investigators led by Brintzinger¹⁸ and Bercaw.¹⁹ Even then, there are elements of this overall process that remain enigmatic, including the requirement for formation of a tertiary alkyl

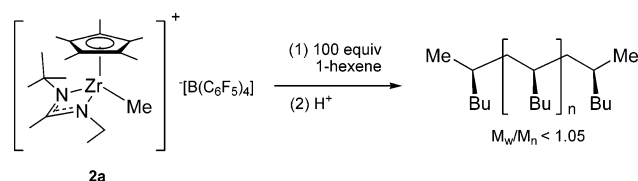
- (11) For late transition-metal living systems, see: (a) Schmidt, G. F.; Brookhart, M. *J. Am. Chem. Soc.* **1985**, *107*, 1443–1444. (b) Brookhart, M.; Volpe, A. F., Jr.; Lincoln, D. M.; Horvath, I. T.; Millar, J. M. *J. Am. Chem. Soc.* **1990**, *112*, 5634–5636. (c) Brookhart, M.; DeSimone, J. D.; Grant, B. E.; Tanner, M. J. *Macromolecules* **1995**, *28*, 5378–5380. (d) Killian, C. M.; Tempel, D. J.; Johnson, L. K.; Brookhart, M. *J. Am. Chem. Soc.* **1996**, *118*, 11664–11665. (e) Ittel, S. D.; Johnson, L. K.; Brookhart, M. *Chem. Rev.* **2000**, *100*, 1169–1204. (f) Gottfried, A. C.; Brookhart, M. *Macromolecules* **2001**, *34*, 1140–1142. (g) Gottfried, A. C.; Brookhart, M. *Macromolecules* **2003**, *36*, 3085–3100.
- (12) (a) Schneider, M. J.; Suhm, J.; Mühlaupt, R.; Prosenic, M.-H.; Brintzinger, H.-H. *Macromolecules* **1997**, *30*, 3164–3168. (b) Deng, L.; Ziegler, T.; Woo, T. K.; Margl, P.; Fan, L. *Organometallics* **1998**, *17*, 3240–3253. (c) Margl, P.; Deng, L.; Ziegler, T. *J. Am. Chem. Soc.* **1999**, *121*, 154–162. (d) Rappé, A. K.; Skiff, W. M.; Casewit, C. J. *Chem. Rev.* **2000**, *100*, 1435–1456. (e) Chirik, P. J.; Bercaw, J. E. *Organometallics* **2005**, *24*, 5407–5423 and references therein.
- (13) Jordan, R. F. *Adv. Organomet. Chem.* **1991**, *32*, 325–387.
- (14) (a) Brookhart, M.; Green, M. L. H.; Wong, L. L. *Prog. Inorg. Chem.* **1988**, *36*, 1–124. (b) Lohrenz, J. C. W.; Woo, T. K.; Fan, L.; Ziegler, T. *J. Organomet. Chem.* **1995**, *497*, 91–104. (c) Cavallo, L.; Guerra, G. *Macromolecules* **1996**, *29*, 2729–2737.

- (15) Kui, S. C. F.; Zhu, N.; Chan, M. C. W. *Angew. Chem., Int. Ed.* **2003**, *42*, 1628–1632.
- (16) (a) Talarico, G.; Busico, V.; Cavallo, L. *Organometallics* **2004**, *23*, 5989–5993. (b) Vanka, K.; Xu, Z.; Ziegler, T. *Organometallics* **2005**, *24*, 419–430.
- (17) (a) Busico, V.; Cipullo, R. *J. Am. Chem. Soc.* **1994**, *116*, 9329–9330. (b) Busico, V.; Cipullo, R. *J. Organomet. Chem.* **1995**, *497*, 113–118.
- (18) (a) Leclerc, M. K.; Brintzinger, H. H. *J. Am. Chem. Soc.* **1995**, *117*, 1651–1652. (b) Leclerc, M. K.; Brintzinger, H. H. *J. Am. Chem. Soc.* **1996**, *118*, 9024–9032. (c) Busico, V.; Caporaso, L.; Cipullo, R.; Landriani, L.; Angelini, G.; Margonelli, A.; Segre, A. L. *J. Am. Chem. Soc.* **1996**, *118*, 2105–2106. (d) Busico, V.; Brita, D.; Caporaso, L.; Cipullo, R.; Vacatello, M. *Macromolecules* **1997**, *30*, 3971–3977.
- (19) Yoder, J. C.; Bercaw, J. E. *J. Am. Chem. Soc.* **2002**, *124*, 2548–2555.
- (20) For an alternative mechanism for chain-end epimerization, see: Resconi, L.; Fait, A.; Piemontesi, F.; Colonna, M.; Rychlicki, H.; Zeigler, R. *Macromolecules* **1995**, *28*, 6667–6676.

Scheme 2



Scheme 3



intermediate through a formal 2,1-reinsertion of the alkene, and the need to still be able to mechanistically account for the observation that switching of the coordinated alkene enantioface can sometimes occur prior to reinsertion without dissociatively losing the alkene to the sea of monomer that is present. Finally, it must be mentioned that isomerizations involving β -hydride eliminations, such as chain-end epimerization, do not appear to be confined only to the polymerization of propene, as extensive end-group analyses by Chien and co-workers²¹ have provided evidence, obtained from metallocene-based 1-hexene polymerizations, for the mechanistically related process of chain-walking of the propagating center back along the polymer backbone and within backbone substituents.

Apart from the few studies performed by the Schrock group, there has been only one other experimental investigation of β -hydride elimination or β -hydride-based isomerizations within cationic early transition metal alkyl complexes that can serve as models for the propagating centers within *living* Ziegler–Natta polymerization systems. In this regard, we have previously reported that dimethyl monocyclopentadienylzirconium acetamidinates of the general structure $(\eta^5\text{-C}_5\text{R}_5)\text{ZrMe}_2[\text{N}(\text{R}^1)\text{C}(\text{Me})\text{N}(\text{R}^2)]$ (**1**) can serve as precursors to the cationic species $\{(\eta^5\text{-C}_5\text{R}_5)\text{ZrMe}[\text{N}(\text{R}^1)\text{C}(\text{Me})\text{N}(\text{R}^2)]\}[\text{B}(\text{C}_6\text{F}_5)_4]$ (**2**) that are highly active initiators for the living polymerization of α -olefins, and in the case of **2a**, where $\text{R} = \text{Me}$, $\text{R}^1 = t\text{-Bu}$, and $\text{R}^2 = \text{Et}$, these polymerizations proceed in a stereospecific fashion as well, according to Scheme 3.⁶ We have further used NMR spectroscopy to observe that, after polymerization, when all monomer has been consumed, the cationic zirconium end-groups of the living polymer species can engage in chain-end-confined chain-walking, albeit at a rate that is orders of magnitude slower than propagation.²² It must also be noted that, while not directly modeling a known living Ziegler–Natta polymerization system, Landis and co-workers²³ have similarly used NMR to directly observe chain-end epimerization within cationic zirconocene polypropenyl species and a *s*-Bu \rightarrow *n*-Bu structural isomerization

within a cationic zirconocene secondary alkyl complex at low temperatures. Accordingly, these observations by us and the Landis group are consistent with the view that it is not that one necessarily needs to avoid β -hydride elimination in order to have a living Ziegler–Natta polymerization within an early transition metal-based system, but rather, it is essential that one avoids chain-release after β -hydride elimination and prior to reinsertion.²⁴

During the course of our extensive mechanistic investigations of living Ziegler–Natta polymerization by the class of initiators encompassed by **2**,⁶ we discovered that the readily available mono- and dialkyl monocyclopentadienylzirconium acetamidinates, **3** and **4**, respectively, are remarkably stable in solution and the solid state, even when the alkyl groups possess β -hydrogens (see Chart 1).²⁵ Indeed, this stability permitted the first successful hydrozirconation of internal alkenes that provides kinetically stable, zirconium-bound secondary (chiral) alkyl groups that are not prone to undergo subsequent structural isomerizations that are the hallmark of products derived from zirconocene-based hydrozirconations.^{26,27} Furthermore, in recently communicated preliminary studies,²² we made additional use of this stability to develop well-defined cationic zirconium complexes bearing alkyl substituents with β -hydrogens that could serve as model compounds for probing chain-walking within living polymers derived from **2**. Now, in the present work, we extend these studies to a wider range of mixed methyl, alkyl complexes, i.e., $\text{R}^1 = \text{Me}$ in **4**, to further investigate the structures and solution stabilities of the corresponding cationic monoalkyl complexes **5** that can be prepared in high yield from **4** through chemoselective methyl group protonolysis employing the borate, $[\text{PhNHMe}_2][\text{B}(\text{C}_6\text{F}_5)_4]$. Incorporation of isotopic labels within *n*-propyl and isobutyl substituents of **5** through the use of the aforementioned hydrozirconation methodology, together with the synthesis and in-depth study of analogous cationic hafnium complexes, including the isotopically labeled isobutyl derivative **6** and the *tert*-butyl derivative **7**, provides additional insights regarding the nature of isomerizations involving β -hydrogen eliminations within this class of group 4 compounds. Importantly, as will be presented, these investigations have produced some intriguing results related to the question of what steric and electronic factors contribute to the living character of polymerizations initiated by **2**. In particular,

(21) Babu, G. N.; Newmark, R. A.; Chien, J. C. W. *Macromolecules* **1994**, *27*, 3383–3388.

(22) Harney, M. B.; Keaton, R. J.; Sita, L. R. *J. Am. Chem. Soc.* **2004**, *126*, 4536–4537.

(23) (a) Sillars, D. R.; Landis, C. R. *J. Am. Chem. Soc.* **2003**, *125*, 9894–9895. (b) Landis, C. R.; Sillars, D. R.; Batterton, J. M. *J. Am. Chem. Soc.* **2004**, *126*, 8890–8891.

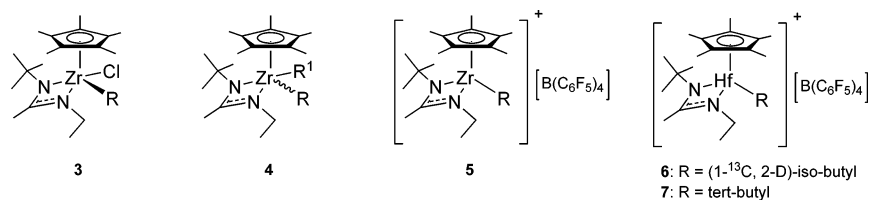
(24) Chain-walking is, in fact, highly competitive with propagation within the living polymerization of α -olefins by the late transition metal initiators described by Brookhart and co-workers.¹¹

(25) Keaton, R. J.; Koterwas, L. A.; Fettingner, J. C.; Sita, L. R. *J. Am. Chem. Soc.* **2002**, *124*, 5932–5933.

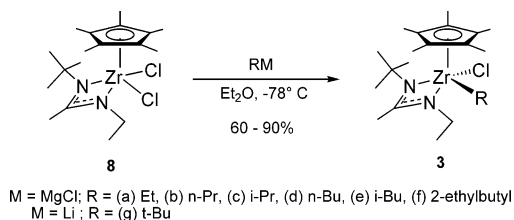
(26) Zhang, Y.; Keaton, R. J.; Sita, L. R. *J. Am. Chem. Soc.* **2003**, *125*, 8746–8747.

(27) Chirik, P. J.; Day, M. W.; Labinger, J. A.; Bercaw, J. E. *J. Am. Chem. Soc.* **1999**, *121*, 10308–10317 and references therein.

Chart 1



Scheme 4



we present the conclusion that the presence of a strong β -hydrogen agostic interaction does not necessarily go hand-in-hand with a low barrier for β -hydride elimination/chain release. Importantly, the results of this work also serve to help delineate the extent to which the cationic alkyl complexes **5** can be used for accurately modeling the corresponding chemistry of the true propagating species involved in living polymerizations initiated by **2a**.

Results

(a) Synthesis of Mixed Halide, Alkyl Complexes 3. As previously reported,²⁵ monoalkylation of the dichloro starting material **8** can be achieved in high yield using alkylmagnesium chloride reagents, or alkyllithium reagents in the case of the sterically demanding *tert*-butyl group, in diethyl ether (Et₂O) at low temperature according to Scheme 4. In the case of the *tert*-butyl derivative **3g**,²⁵ it is imperative that much longer reaction times (~10 h) at -78°C be used since the large amount of *tert*-butyllithium still remaining at short reaction times serves to isomerize the zirconium-bound *tert*-butyl group to an isobutyl group upon warming the reaction mixture to room temperature (cf. ~100% yield of the isobutyl derivative **3e** after 1 h vs a 9:1 ratio of **3g** and **3e** after 10 h). Fortunately, the small amount of **3e** that is still produced can be removed by fractional crystallization to provide analytically pure **3g** that is then indefinitely stable in solution. Indeed, all the derivatives of **3** shown in Scheme 4 are stable in solution and in the solid state at room temperature, thereby greatly facilitating their full characterization by spectroscopic and analytical means.

As a side note, when alkylmagnesium *bromide* reagents are used in Scheme 4, transhalogenation at zirconium occurs to provide the monoalkylated product as a mixture of bromo and chloro derivatives. Although this halide mixture can be used in subsequent alkylation reactions, we have found it to be inconvenient with respect to obtaining clean spectroscopic data and unequivocal chemical analysis data. The one instance where it has proven to be useful, however, is in obtaining crystal structures through single-crystal X-ray analysis, where the bromo derivatives are oftentimes more likely to produce high-quality single crystals than the chloro derivatives.

Regarding crystal structures, a number have been obtained for derivatives of **3**, or as the corresponding bromide compound, and some of these have been previously reported.^{22,25} Figure 1

displays the molecular structures of the isopropyl and *tert*-butyl derivatives, **3c** and **3g**, respectively, along with those for the bromo, alkyl analogues of **3e** and **3f**. Significantly, in all of the structures studied so far, the alkyl substituent is always directed toward the *N*-Et substituent of the acetamidinate fragment, as depicted in Scheme 4. Furthermore, as illustrated by the structure of the bromo analogue of **3f**, the steric bulk of large alkyl substituents appears to be accommodated by “tucking-in” part of the alkyl fragment beneath the acetamidinate moiety. Surprisingly, none of the structures display any unusual geometries as a result of strong nonbonded steric interactions, and this includes that of the *tert*-butyl derivative **3g**. With respect to geometric parameters, the only bond lengths of particular note are the zirconium–nitrogen bonds, which will be discussed in more detail shortly. Finally, in none of the crystal structures for chloro, alkyl derivatives of **3** has there ever been observed any interaction between the metal and the β -hydrogens of the alkyl substituent.

In solution, ¹H NMR spectroscopy reveals that all the chloro, alkyl derivatives of **3** appear to exist as a single diastereomer, which is assumed to be the same as that depicted in Scheme 4 and which is found in all the crystal structures obtained to date. In addition, variable-temperature NMR provides evidence that all of these compounds are *configurationally stable* on the NMR time frame with respect to racemization through “amidinate ring-flipping”²⁸ that occurs through metal-centered epimerization. Finally, variable-temperature NMR was also used to verify that, at elevated temperatures up to 80°C , the isopropyl derivative **3c** does not isomerize to the *n*-propyl derivative **3b**, nor does the *tert*-butyl derivative **3g** isomerize to the isobutyl derivative **3e**. This high degree of stability toward isomerization through a presumed β -hydride elimination/reinsertion mechanism stands in sharp contrast to the observations with zirconocene-based secondary and tertiary chloro, alkyl complexes.²⁷

(b) Synthesis of Mixed Methyl, Alkyl Complexes 4. As Scheme 5 shows, methylation of **3** using methyl lithium at -78°C in Et₂O provided the desired mixed methyl, alkyl complexes **4** in good to excellent isolated yields, depending upon their ease of crystallization. The only case where this procedure failed completely was in the attempted methylation of the *tert*-butyl derivative **3g**. In fact, all attempts to methylate **3g** through a variety of different reagents, e.g., MeLi, MeMgCl, ZnMe₂, and AlMe₃, and under different conditions, failed to produce the desired *tert*-butyl, methyl derivative of **4**, presumably due to the large degree of steric shielding of the metal center that the *tert*-butyl group provides. Under forcing conditions (e.g., elevated temperatures or excess MeLi), only isomerization to the isobutyl derivative **4e** was observed, and curiously, switching the order of reagents for the synthesis from the dichloride **8**,

(28) (a) Sita, L. R.; Babcock, J. R. *Organometallics* **1998**, *17*, 5228–5230. (b) Koterwas, L. A.; Fettinger, J. C.; Sita, L. R. *Organometallics* **1999**, *18*, 4183–4190.

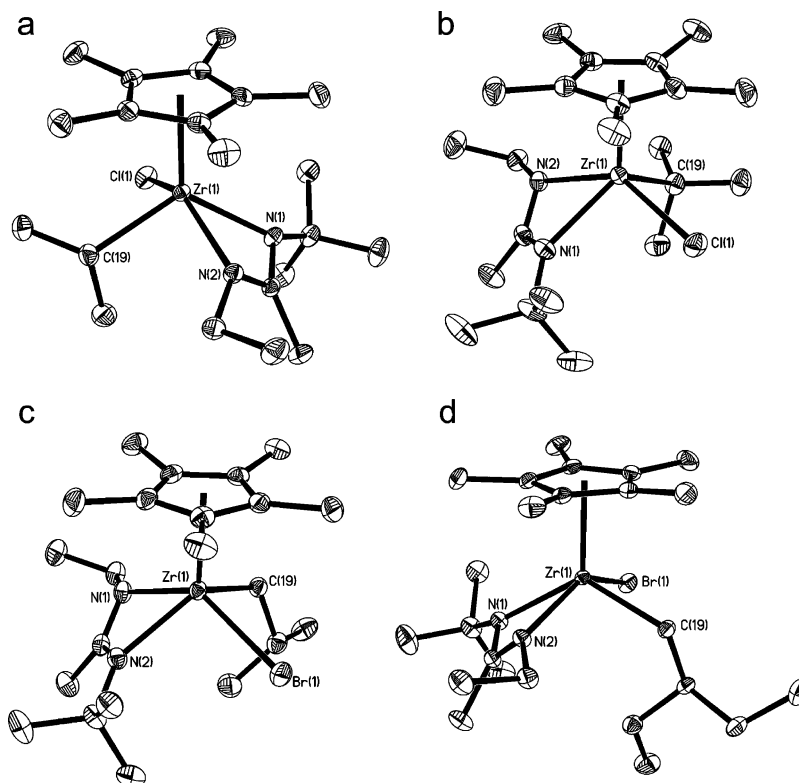
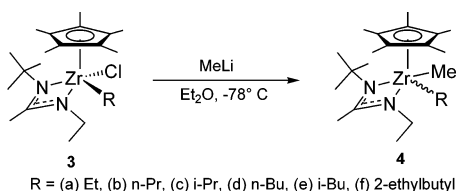


Figure 1. Molecular structure (30% thermal ellipsoids) of (a) **3c**, (b) **3g**, (c) **3e** (Br analogue), and (d) **3f** (Br analogue) with partial atom labeling. Hydrogen atoms have been removed for the sake of clarity.

Scheme 5



i.e., methyllithium, followed by *tert*-butyllithium, also failed to yield the desired mixed methyl, *tert*-butyl product.

As with the mixed chloro, alkyl complexes **3**, all the mixed methyl, alkyl derivatives of **4** were found to be stable in solution and in the solid state at room temperature, and all could be recrystallized to an analytically pure state as determined by ^1H NMR spectroscopy. However, whereas all the derivatives of **3** gave satisfactory chemical analyses, the dialkyl compounds often failed to provide similarly conclusive microanalysis data, even after repeated attempts, presumably due to various decomposition pathways that are available at moderate temperatures.^{25,29} Accordingly, in those cases, single-crystal X-ray analysis was performed to verify composition, and Figure 2 provides the molecular structures obtained for some of the more interesting examples. As can be seen, in keeping with the structures of Figure 1, the structures for **4a,c–e** all adopt a configuration that places the alkyl substituent on the same side as the *N*-Et group of the acetamidinate fragment, and once again, no interactions of β -hydrogens with the metal center are observed in the solid state. With respect to geometrical parameters, it is important to note that between the chloro (bromo), alkyl derivatives of **3** and the methyl, alkyl derivatives of **4**, the latter class uniformly has longer zirconium–nitrogen bonds. For

example, the Zr–N bond lengths of the chloro, isopropyl compound **3c** are 2.2419(11) Å for Zr(1)–N(2) and 2.2528(11) Å for Zr(1)–N(1), whereas the corresponding values in the methyl, isopropyl derivative **4c** are 2.2594(9) and 2.2808(9) Å, respectively. Although these Zr–N bond differences between **3** and **4** would, at first glance, appear to be small, they are likely the origin of the dramatic difference in solution configurational stability displayed by the two classes of compounds (*vide infra*).

In solution, ^1H NMR spectra suggest that all derivatives of **4** are *configurationally unstable* with respect to amidinate ring-flipping, and as depicted by Scheme 6, at room temperature, they exist as a mixture of two interconverting diastereomers, the relative ratio of which depends on the steric bulk of the zirconium-bonded alkyl group. Indeed, for the isobutyl derivative **4e**, it was recently determined, through the use of 2D ^{13}C - $\{^1\text{H}\}$ EXSY NMR, that metal-centered epimerization is a facile process, even at $-10\text{ }^\circ\text{C}$.^{6f} It is not surprising, then, that this dynamic process presumably allows for the major diastereomer of **4** to be obtained as the single crystalline product in each case. More importantly, it is most probable that the observed difference in configurational stability between the chloro, alkyl derivatives of **3** (stable) and the methyl, alkyl derivatives of **4** (unstable) is due to the relative electronic effects associated with the chloro and alkyl substituents. In other words, given the greater electronegativity of the chloro group, the zirconium–nitrogen interactions in **3** are potentially stronger than in **4**, and these are manifested not only in shorter Zr–N bond distances but also in a larger energy barrier for amidinate ring-flipping. Finally, it can be noted that this difference in configurational stability of **3** and **4** is more than just of cursory interest, in that it can be used to direct stereocontrol during the polymerization

(29) Keaton, R. J.; Sita, L. R. *Organometallics* **2002**, *21*, 4315–4317.

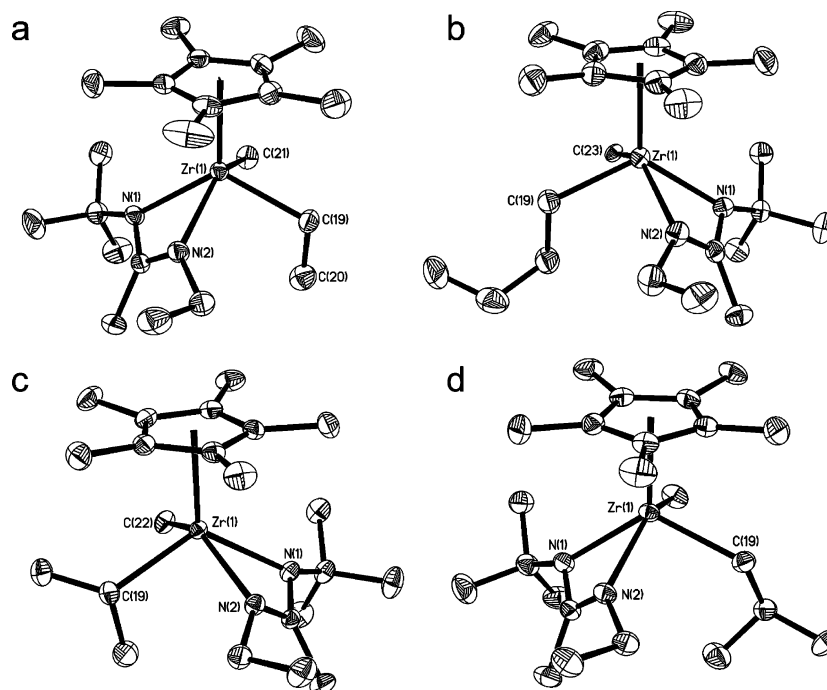
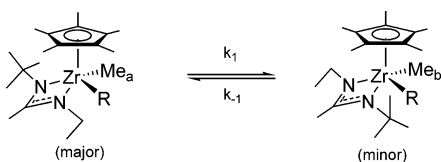
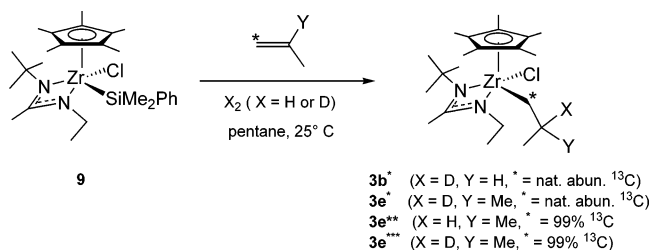


Figure 2. Molecular structure (30% thermal ellipsoids) of (a) **4a**, (b) **4d**, (c) **4c**, and (d) **4e** with partial atom labeling. Hydrogen atoms have been removed for the sake of clarity.

Scheme 6



Scheme 7

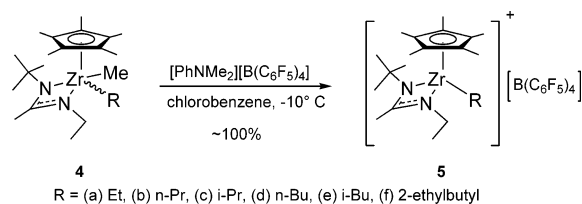


of α -olefins by newly discovered chloride and methyl group degenerative-transfer living Ziegler–Natta polymerizations based on **1–3**.^{6f,g}

(c) Synthesis of Isotopically Labeled Derivatives of **3** and **4**

To better investigate structural isomerizations involving β -hydride elimination/reinsertion, it was desirable to have isotopically labeled derivatives of **3** and **4** in which the isotopic label could be placed at either an α - or β -position within an alkyl substituent with known certainty. Fortunately, the newly devised hydrozirconation chemistry shown in Scheme 7 provided a convenient route to several of these compounds.^{22,26} Thus, hydrogenolysis of the chloro, silyl complex **9** using either H_2 or D_2 generates the chloro hydride (deuteride) zirconium species, $(\eta^5\text{-C}_5\text{Me}_5)\text{Zr}(\text{Cl})(\text{X})[\text{N}(\text{t-Bu})\text{C}(\text{Me})\text{N}(\text{Et})]$ (X = H or D), that in the presence of an excess of either propene or $[1\text{-}^{13}\text{C}]2$ -methylpropene engages in hydrozirconation to provide in high yield (1) the singly labeled *n*-propyl derivative **3b*** that has D in the β -position, (2) the isobutyl derivative **3e*** that is similarly singly labeled in the β -position, (3) singly labeled **3e****

Scheme 8



with ^{13}C in the α -position, and finally, (4) doubly labeled **3e***** that has ^{13}C in the α -position and D in the β -position. In the case of **3b***, it is important to note that hydrozirconation does not proceed in a highly stereoselective fashion, and therefore, a $\sim 3:1$ mixture of diastereomers (with respect to the relative configuration of the metal and β -carbon centers) is produced. As will be related shortly, this mixture of diastereomers for **3b*** has no consequences for the results obtained. It is also important to note that variable-temperature ^1H NMR was used to confirm that no scrambling of the isotopic labels occurs in these derivatives of **3b** and **3e**, even at elevated temperatures of up to at least 80°C . Finally, following the standard synthetic protocol, the corresponding isotopically labeled methyl, alkyl derivatives, **4b***, **4e***, **4e****, and **4e*****, were obtained, and once again, variable-temperature ^1H NMR was used to confirm that the isotopic labels remain intact within the alkyl substituents, even at elevated temperatures.

(d) Synthesis of Cationic Complexes **5 via Chemoselective Methyl Group Protonolysis.** As depicted in Scheme 8, it was discovered that a range of derivatives of **5** can be prepared in virtually quantitative yield through chemoselective protonolysis of the methyl group of **4** using 1 equiv of $[\text{PhNMe}_2][\text{B}(\text{C}_6\text{F}_5)_4]$ when this reaction is conducted at -10°C using chlorobenzene as the solvent. To determine just how chemoselective this process is, a ^{13}C -methyl-labeled derivative of **4e** was prepared from **3e** using $^{13}\text{CH}_3\text{Li}$ (99% ^{13}C) as the alkylating reagent. Protonolysis of this compound employing $[\text{PhNMe}_2][\text{B}(\text{C}_6\text{F}_5)_4]$

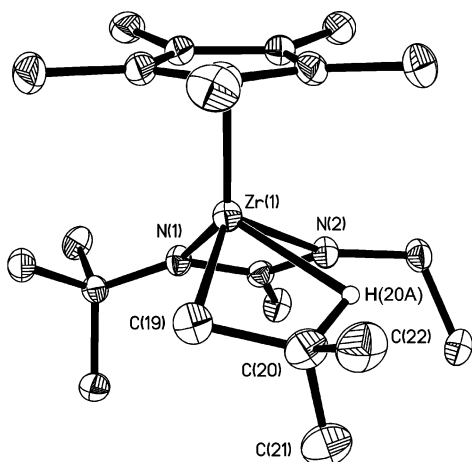


Figure 3. Molecular structure (30% thermal ellipsoids) of **5e** with partial atom labeling. The $[B(C_6F_5)_4]^-$ anion and hydrogen atoms, except the crystallographically located β -hydrogen, have been removed for the sake of clarity.

was then carried out as described, and the resulting cationic zirconium species was immediately used as an initiator for the living polymerization of 1-hexene at -10°C . GPC subsequently confirmed that the molecular weight of the resulting isotactic poly(1-hexene) was in agreement with quantitative generation of a cationic initiator, and ^{13}C NMR analysis of this polymeric material confirmed the absence of any incorporation of the ^{13}C -methyl label into the end-groups, thereby confirming that only the cationic isobutyl derivative **5e** was initially produced by the procedure of Scheme 8.^{6f}

Although it has been exceedingly difficult to obtain single crystals of derivatives of **5**, in the case of the isobutyl derivative **5e**, this feat could be reproducibly achieved at -30°C by layering pentane on top of a chlorobenzene solution, all within an NMR tube (~ 20 mg of **5e** in 0.5 mL of chlorobenzene and 1 mL of pentane). Figure 3 presents the molecular structure of **5e** as obtained by X-ray crystallography. Within this structure, the borate counterion (not shown) is well displaced from the zirconium cation, and there are no close Zr–F interactions between the ion pair. Of immediate interest is the position of the crystallographically located hydrogen atom, H(20A), that puts it into a β -agostic interaction with the zirconium center [cf. Zr(1)–H(20A) distance of 2.25(3) Å].³⁰ Additional evidence for this β -hydrogen agostic interaction is provided by the observation that the β -carbon atom, C(20), is more pyramidalized toward planarity than tetrahedral, as supported by the sum of the bond angles for C(19)–C(20)–C(21), C(19)–C(20)–C(22), and C(21)–C(20)–C(22), which is 337.7° (cf. 328° and 360° expected for idealized tetrahedral and planar geometries, respectively). It is also interesting to note that the zirconium–nitrogen bonds in the cation **5e** are very short, at 2.1376(18) and 2.1882(18) Å, and so it would appear that this geometric parameter is indeed a good measure of the electron deficiency of the metal center, as now established by the zirconium–nitrogen bond length trend: **5e** > **3e** > **4e**.^{6c}

In solution, all of the cations **5a–f** are remarkably stable at -10°C , thus allowing their solution structures to be probed by a variety of NMR techniques at this and other temperatures. Importantly, although a mixture of diastereomers of **4** is used

to generate **5**, in each case, only a single, configurationally stable species for **5** is observed in solution. This configurational stability with respect to metal-centered epimerization is in keeping with the greater electron deficiency of the metal and, hence, the shorter (stronger) Zr–N interactions with the amidinate fragment (vide supra).

Given the β -hydrogen agostic interaction observed in the solid-state structure of **5e**, this compound served as a good starting point to look for similar agostic interactions in solution. Figure 4 presents the ^1H NMR spectrum of the cation **5e** recorded in chlorobenzene- d_5 at -10°C , and the resonance of particular note is that appearing at -0.27 ppm. Unequivocal assignment of this resonance as being that of the β -hydrogen of the isobutyl group was made through a 2D ^1H – ^1H COSY NMR experiment that also established that the two resonances appearing at 0.77 and 1.59 ppm as a pair of doublet of doublets (dd) are for the two diastereomeric α -hydrogens of this same fragment. Although the significant upfield chemical shift for the β -hydrogen is already suggestive of an agostic interaction with the metal center,¹⁴ more compelling evidence was provided by the value of 96 Hz for the associated $^1J(^{13}\text{C}_\beta\text{–}^1\text{H}_\beta)$ coupling constant, which was conveniently obtained from a 2D J -resolved ^{13}C – ^1H HSQC NMR spectrum. More specifically, the substantial reduction in this coupling constant relative to a standard, unperturbed $^1J(^{13}\text{C}\text{–}^1\text{H})$ value of 125 Hz signifies a weaker $\text{C}_\beta\text{–H}_\beta$ interaction, as expected if the β -hydrogen is engaged in a strong agostic interaction with the metal center.¹⁴ The 2D J -resolved ^{13}C – ^1H HSQC NMR method, however, also simultaneously provides $^1J(^{13}\text{C}\text{–}^1\text{H})$ values for the other protons of the alkyl fragment, and in the case of **5e**, those of interest are for the α -hydrogens, with $^1J(^{13}\text{C}_\alpha\text{–}^1\text{H}_\alpha)$ values of 128 and 138 Hz. Finally, a series of 1D NOE difference NMR spectra confirmed that the solution structure of **5e** is indeed the same as that in the solid state, namely, that the β -hydrogen agostic interaction occurs on the N -ethyl side of the amidinate, as shown in Figure 4.

Table 1 provides solution $^1J(^{13}\text{C}_\alpha\text{–}^1\text{H}_\alpha)$ and $^1J(^{13}\text{C}_\beta\text{–}^1\text{H}_\beta)$ values for other derivatives of **5** that were obtained in a similar fashion. Interestingly, except for the ethyl derivative **5a**, for which a β -hydrogen agostic interaction with the freely rotating β -methyl group cannot be unequivocally established at -10°C , all the $^1J(^{13}\text{C}_\beta\text{–}^1\text{H}_\beta)$ values of Table 1 are supportive of a strong β -hydrogen agostic interaction with the metal center. Furthermore, 1D NOE difference NMR confirms the solution structure of all of these derivatives to be the same as that of **5e**, in which the β -hydrogen agostic interaction occurs on the N -ethyl side of the amidinate fragment. It is also interesting to note that, in the case of the isopropyl derivative **5c**, only one of the diastereomeric β -methyl groups is clearly engaged in a β -hydrogen agostic interaction, while the other is not.

(e) Synthesis of the Hafnium Complexes 6 and 7. We have recently reported that the cationic methyl and isobutyl hafnium analogues of **2a** and **5e** can also serve as initiators for the isospecific living polymerization of 1-hexene, albeit with a rate of propagation that is ~ 60 times slower than that observed with their second-row cousins.^{6h} Given this, it was decided to expand the range of the present studies to include a study of isomerization within the isotopically labeled cationic hafnium isobutyl derivative **6**. Furthermore, considering all the previous failed attempts to prepare a cationic *tert*-butyl derivative of **5**, it was

(30) Jordan, R. F.; Bradley, P. K.; Baenziger, N. C.; LaPointe, R. E. *J. Am. Chem. Soc.* **1990**, *112*, 1289–1291.

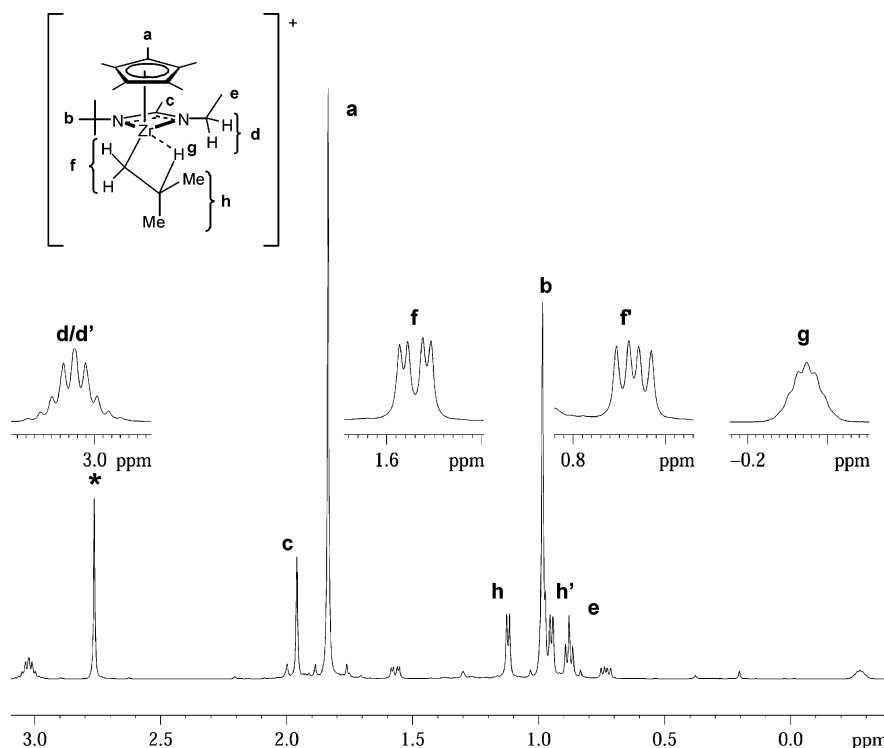


Figure 4. ^1H NMR (400 MHz, $\text{C}_6\text{D}_5\text{Cl}$, -10°C) spectrum of **5e**. The resonance marked with an asterisk is for the methyl groups of PhNMe_2 .

Table 1. $^1\text{J}(^{13}\text{C}-^1\text{H})$ Coupling Constants for the R Group in **5^a**

R	$^1\text{J}(^{13}\text{C}_\alpha-^1\text{H}_\alpha)^b$	$^1\text{J}(^{13}\text{C}_\beta-^1\text{H}_\beta)^b$	
Et (5a)	140	135	123
n-Pr (5b)	144	133	110
i-Pr (5c)	155	126	85
n-Bu (5d)	140	133	121
i-Bu (5e)	138	128	92
2-Et-Bu (5f)	140	120	86

^a Obtained from 2D $^{13}\text{C},^1\text{H}$ HSQC NMR in chlorobenzene- d_5 at -10°C . ^b Two values denote that two distinct resonances for diastereotopic protons were observed.

felt that better success might be achieved in efforts to synthesize the corresponding cationic hafnium *tert*-butyl species **7**.

To begin, the synthesis of doubly isotopically labeled **6** was achieved in a fashion analogous to the synthetic protocol used to prepare the zirconium analogue **5e*****. Thus, as Scheme 9 reveals, hydrogenolysis of the chloro, silyl hafnium complex **10** under a D_2 atmosphere resulted in the hydrohafnation³¹ of $[1-^{13}\text{C}]2$ -methylpropene to provide the desired isotopically labeled chloro, isobutyl hafnium compound **11**, albeit in only moderate yield as compared to the analogous hydrozirconation reaction (cf. 70% yield for **3e***** vs 48% for **11**). Methylation of **11** using the standard procedure uneventfully provided the isotopically labeled methyl, isobutyl hafnium compound **12**. Finally, treatment of **12** with 1 equiv of $[\text{PhNHMe}_2][\text{B}(\text{C}_6\text{F}_5)_4]$ in chlorobenzene at -10°C provided the desired cationic species **6** in quantitative fashion as determined by ^1H NMR. In this respect, it is important to note that it was previously reported that *no evidence for a β -hydrogen agostic interaction* could be found for unlabeled **6** in solution using 1D and 2D NMR techniques.^{6h}

Regarding the synthesis of **7**, the first attempt involved alkylation of the dichloro hafnium starting material **13**^{6h} with

tert-butyllithium to provide the chloro, *tert*-butyl product **14** according to Scheme 10. Single-crystal X-ray analysis confirmed the structure of **14**, which is very similar to that previously reported for the zirconium analogue **3g**.^{25,32} However, attempts to methylate **14** produced only the unlabeled derivative of the methyl, isobutyl compound **12**. Fortunately, reversing the order of alkylation of **13** was successful. Thus, as Scheme 10 shows, methylation of **13** using methylmagnesium chloride first provided the chloro, methyl compound **15**, which was then reacted with *tert*-butyllithium overnight at -55°C to afford the elusive methyl, *tert*-butyl complex **16**. Finally, upon treatment of **16** with 1 equiv of $[\text{PhNHMe}_2][\text{B}(\text{C}_6\text{F}_5)_4]$, the desired cationic *tert*-butyl hafnium complex **7** was quantitatively generated, as determined by ^1H NMR spectroscopy.

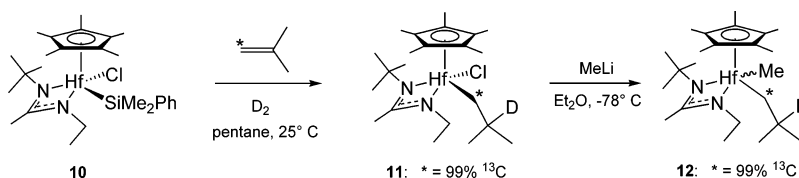
(f) Decomposition and Isomerization of Cationic Zirconium and Hafnium Complexes. As mentioned previously, all derivatives of cationic zirconium **5** appear to be extremely stable at -10°C , with no detectable amount of decomposition or isomerization (where applicable) being observed by ^1H NMR after ~ 18 h. At the higher temperature of 30°C , however, decomposition does ensue, and an initial screening qualitatively determined a relative order of stability of **5** to be $\text{R} = \text{Et} > \text{n-Pr} > \text{n-Bu} > \text{i-Pr} > \text{i-Bu} > 2\text{-ethylbutyl}$. Furthermore, in keeping with our past observations,^{3h,33} the main metal-containing product isolated from these decompositions, and oftentimes in high yield, is the dichloro dication species, $\{\eta^5\text{-C}_5\text{Me}_5\text{Zr}(\mu\text{-Cl})[\text{N}(\text{Et})\text{C}(\text{Me})\text{N}(\text{t-Bu})]\}_2[\text{B}(\text{C}_6\text{F}_5)_4]_2$, shown in Scheme 11, that presumably arises from chloride abstraction from the chlorobenzene solvent and for which a crystal structure has been obtained.³⁴ Similar μ -chloro dicationic dizirconium complexes have been previously reported to form in halogenated

(32) Detailed information is provided in the Supporting Information.

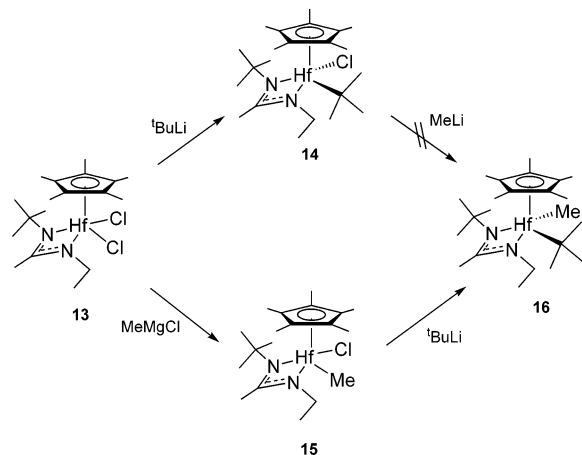
(33) Zhang, Y.; Reeder, E. K.; Keaton, R. J.; Sita, L. R. *Organometallics* **2004**, *23*, 3512–3520.

(31) Erker, G.; Schlund, R.; Krüger, C. *Organometallics* **1989**, *8*, 2349–2355.

Scheme 9



Scheme 10



solvents starting from cationic zirconium methyl species.³⁵ In the present case, we believe the reactivity of the solvent with any metal hydride intermediates that might be formed upon β -hydride elimination in **5**, thereby providing the dichloro dication, may be precluding the ability to directly observe and isolate these species.

On the basis of the preliminary screen, several derivatives of **5** were targeted for more in-depth analysis, with the subset being comprised of **5b** (R = *n*-Pr), **5c** (R = *i*-Pr), **5e** (R = *i*-Bu), and **5f** (R = 2-ethylbutyl) (see Chart 2). Importantly, as presented earlier, all of these cationic complexes appear to engage in a strong β -hydrogen agostic interaction in solution as depicted.

At 0 °C, both the isobutyl and 2-ethylbutyl derivatives, **5e** and **5f**, respectively, were observed to decompose in a first-order fashion, while the *n*-propyl and isopropyl derivatives, **5b** and **5c**, respectively, remained unchanged. Surprisingly, the more sterically encumbered derivative, **5f**, decomposed approximately twice as fast as the isobutyl derivative **5e** ($k_d = 0.067 \text{ h}^{-1}$; $t_{1/2} = 10.3 \text{ h}$ vs 0.034 h^{-1} ; 20.4 h , respectively). To put these absolute and relative rates of decomposition for **5e** and **5f** into proper perspective with respect to the living polymer species derived from **2a**, for which **5e** and **5d** had been hoped from the start to serve as viable models, the rate of decomposition for the living polymer derived from the polymerization of 1-decene was also determined at 0 °C at the same concentration of cationic zirconium species. To achieve this, [1- ^{13}C]1-decene (99% ^{13}C) was first oligomerized in living fashion in chlorobenzene- d_5 at -10 °C to a degree of polymerization (DP) of ~ 15 by judiciously setting the ratio of the monomer concentration to that of the initiator **2a** (DP = [M]/[I] for living polymerizations). After equilibration of the living poly(1- ^{13}C -

decene) (LPD) sample at 0 °C, disappearance of the zirconium-bonded α -carbon ^{13}C resonance for this material at 82.3 ppm^{6c} was then followed by inverse-gated ^{13}C NMR spectroscopy. Once again, decomposition of this LPD was seen to occur in first-order fashion at 0 °C, to provide a k_d of 0.22 h^{-1} ($t_{1/2} = 3.2 \text{ h}$), a value that is more than 6 times greater than that of the isobutyl derivative **5e**.

Additional insight into the nature of the processes by which **5e** decomposes was obtained by observing the course of decomposition of the singly deuterium-labeled derivative **5e*** and the doubly isotopically labeled derivative **5e*****. Thus, through the use of ^1H NMR, it was first determined that, concurrent with decomposition, the original β -positioned deuterium label of **5e*** begins to undergo scrambling within the isobutyl group almost immediately upon warming from -10 to 0 °C, with this process reaching apparent equilibrium in approximately 11 h. In the case of **5e*****, when decomposition and scrambling was followed by ^{13}C NMR, 1:1:1 triplets for two diastereotopic $^{13}\text{CH}_2\text{D}$ -labeled methyl groups of the isobutyl substituent were observed, with no evidence being obtained for the corresponding singlets that should arise from formation of singly ^{13}C -labeled methyl groups (see Figure 5). In other words, the mechanism by which scrambling occurs always places a D and ^{13}C label on the same carbon atom, as shown in Scheme 12, and this is consistent with the multistep sequence of events also shown in this scheme that is identical in nature to the mechanism proposed by Busico and co-workers¹⁷ for chain-end epimerization.

A few other comments regarding the isomerization/decomposition of **5e***** are in order. First, as Figure 5 reveals, in addition to the 2-methylpropene product expected from β -hydrogen elimination, formation of 2-methylpropane (isobutane) was also observed to occur both initially and continuously throughout decomposition. Initially, [1- ^{13}C ,2-D]2-methylpropane is predominately produced from the presumed protonolysis of the unscrambled isobutyl fragment, but near the end of decomposition/isomerization, increasing amounts of [1- ^{13}C ,1-D]2-methylpropane are generated from protonolysis of the isomerized isobutyl group in **5e*****, as observed in Figure 5. Schrock and co-workers^{4g} previously reported formation of 2-methylpropane during decomposition of their isobutyl hafnium initiator, but they attributed this product to the reaction of the initiator with dimethylaniline, which was present in their system as in ours, being the byproduct of using [PhNHMe₂][B(C₆F₅)₄] to initially form a cationic species through protonolysis. In the present study, replacing this borate with [Ph₃C][B(C₆F₅)₄], which can also be used to chemoselectively generate **5** from **4** through methide abstraction, unfortunately did not obviate production of 2-methylpropane during decomposition of **5e**, nor did any other attempts to remove obvious proton sources from the equation (e.g., use of silylated glassware). Given the strict first-order decomposition of **5e** at different concentrations, we are accordingly led to believe that formation of the saturated

(34) Full characterization and crystallographic analysis will be presented elsewhere as part of a structural study of the series $\{(\eta^5\text{-C}_5\text{Me}_5)\text{Zr}(\mu\text{-X})\text{[N(Et)C(Me)N(t-Bu)]}_2\text{[B(C}_6\text{F}_5)_4]_2$ (X = F, Cl, Br, Me).

(35) (a) Gomez, R.; Green, M. L. H.; Haggitt, J. L. *J. Chem. Soc., Dalton Trans.* **1996**, 939–946. (b) Vollmerhaus, R.; Rahim, M.; Tomaszewski, R.; Xin, S.; Taylor, N. J.; Collins, S. *Organometallics* **2000**, *19*, 2161–2169.

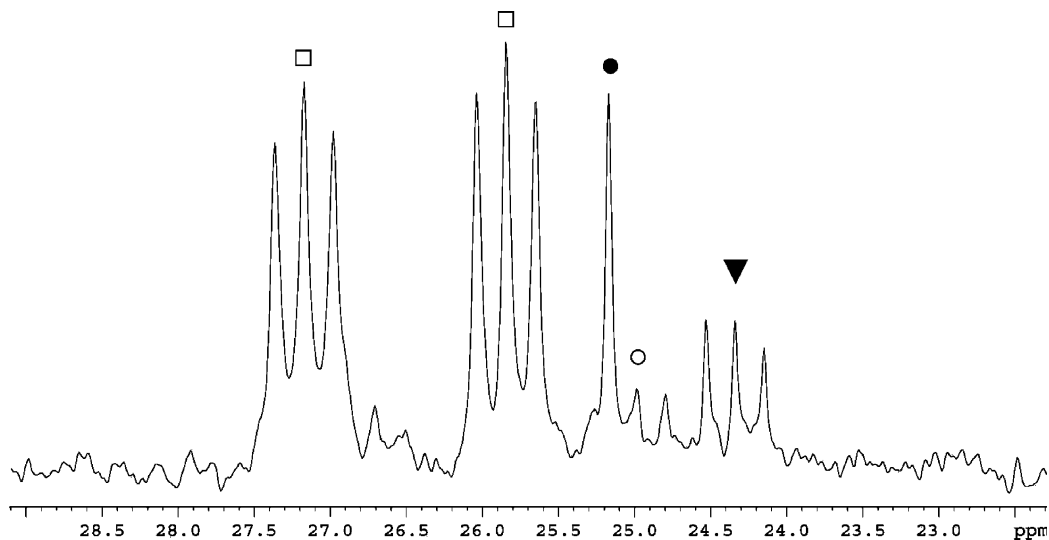


Figure 5. $^{13}\text{C}\{^1\text{H}\}$ NMR (100 MHz, $\text{C}_6\text{D}_5\text{Cl}$, 0 °C) of **5e***** after 15 h at 0 °C. □, diastereotopic doubly labeled methyl groups ($^{13}\text{CH}_2\text{D}$) of the isobutyl moiety; ●, $\text{DC}(\text{CH}_3)_2(^{13}\text{CH}_3)$; ○, $\text{HC}(\text{CH}_3)_2(^{13}\text{CH}_2\text{D})$; ▼, $\text{H}_2\text{C}=\text{C}(\text{CH}_3)(^{13}\text{CH}_2\text{D})$.

Scheme 11

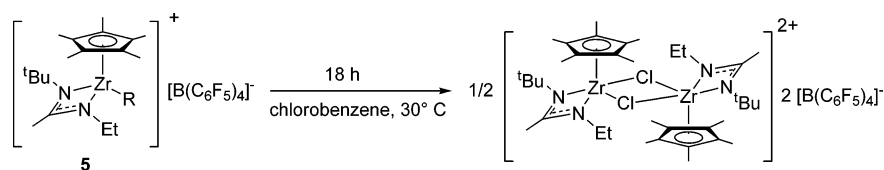
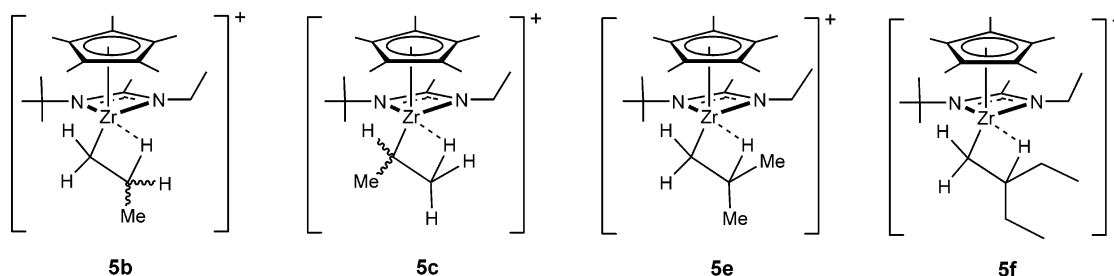
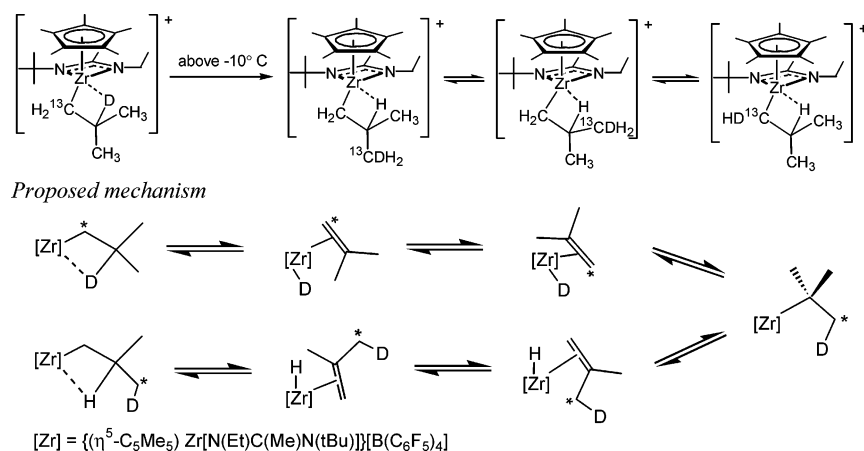


Chart 2



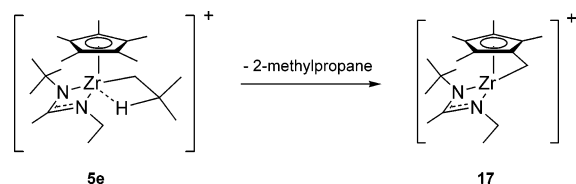
Scheme 12



hydrocarbon coproduct of decomposition of this species is due to a competitive first-order intramolecular process. As shown in Scheme 13, the most likely decomposition path leading to 2-methylpropane from **5e** involves intramolecular H-abstraction from one of the methyl groups of the cyclopentadienyl ligand to produce the cationic “tuck-in” metal species **17**, which can

reasonably be assumed to be highly reactive. Indeed, much precedent exists in the literature for a transformation such as that shown.³⁶ Efforts are currently underway to unequivocally substantiate this decomposition pathway, as it clearly has possible relevance to attempts to utilize the initiators **2** at temperatures well above that which has previously been shown

Scheme 13



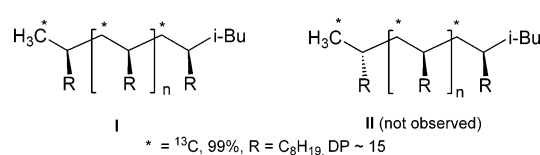
to provide clear living character in the polymerizations of higher α -olefins (e.g., $-10\text{ }^\circ\text{C}$ in the case of 1-hexene).

A second point regarding the isomerization/decomposition of **5e** is that, assuming β -hydride elimination to be the rate-determining step for isomerization, 1,2-reinsertion to regenerate unscrambled **5e***** and isomerization of the isobutyl group involving a *tert*-butyl intermediate through a 2,1-reinsertion according to Scheme 12 must both be very facile processes that effectively compete extremely well with irreversible chain-release from alkene hydride intermediates. Indeed, scrambling of isotopic labels in **5e***** appears immediately by ^{13}C NMR at $0\text{ }^\circ\text{C}$ at a point when minimal loss of compound (decomposition) has yet occurred. No NMR spectroscopic evidence for such a cationic *tert*-butyl intermediate (i.e., the hitherto unattained **5g**), however, has yet been obtained. More disappointingly, all attempts to identify a reagent that could be used to chemically trap the presumed but unobserved-as-of-yet alkene hydride intermediates in order to eliminate the reversibility of the β -hydride elimination process and isotopic scrambling, and thereby permit kinetic analyses to obtain clear-cut thermodynamic parameters, including a kinetic isotope effect, have failed to produce a viable candidate as of yet.

In the case of the 2-ethylbutyl derivative **5f**, a large-scale (100 mg) decomposition at $0\text{ }^\circ\text{C}$ provided a volatile hydrocarbon product that contained not only the expected 2-ethyl-1-butene from direct β -hydride elimination but also small amounts of 3-methyl-1-pentene and (*E/Z*)-3-methyl-2-pentene that more detailed spectroscopic studies have revealed most likely arise from chain-walking through a series of β -hydride elimination/alkene rotation/reinsertion sequences that are identical in nature to those of chain-end epimerization. As before, a significant amount of the saturated hydrocarbon, 2-ethylbutane, was also obtained through presumed competitive intramolecular H-abstraction from a methyl group of the cyclopentadienyl ligand according to Scheme 13.

As previously mentioned, end-group-confined chain-walking has been directly observed by us in living cationic zirconium poly(1-butenyl) (LPB) (DP ≈ 15) at $-10\text{ }^\circ\text{C}$,²² a temperature at which the isobutyl derivative **5e***** does not engage in isotope label scrambling, and at which both **5e** and the 2-ethylbutyl derivative **5f** are indefinitely stable. Thus, the conclusion reached from these observations is that living polymers derived from the polymerization of higher α -olefins (i.e., 1-butene, 1-hexene, etc.) possess a lower barrier to β -hydride elimination, and hence chain-walking, relative to the model compounds **5e** and **5f**, despite evidence for strong β -hydrogen agostic interactions in solution for the latter two in contrast to no evidence as of yet

Chart 3

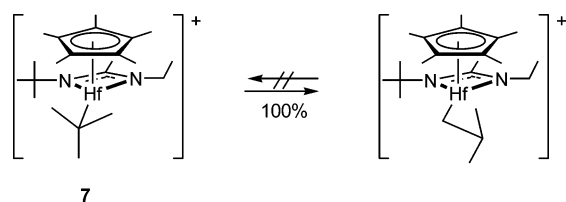


for a similar β -hydrogen agostic interaction being observed by NMR techniques for the LPB. In addition to these chain-walking studies with living polymeryl species, further efforts were made to determine whether such species can engage in chain-end epimerization, which in the case of living polymers derived from higher α -olefins (i.e., other than propene) must occur through a process involving enantiofacial switching of the coordinated olefin within an alkene hydride intermediate. Thus, using the isobutyl compound **5e** as an initiator in order to place an isobutyl group at one end of the polymer chain, isotactic LPD (DP ≈ 15) was once again produced at $-10\text{ }^\circ\text{C}$ and allowed to gestate at this temperature for 18 h, during which time aliquots were periodically taken and acid-quenched to produce a ^{13}C -labeled methyl end-group where the metal had been attached. As it has previously been determined by us that two distinct ^{13}C NMR resonances exist for the two possible diastereomers **I** and **II** shown in Chart 3, if chain-end epimerization of the LPD were occurring over time, then the ^{13}C NMR spectra for the aliquots should show the appearance and growth of a new ^{13}C -labeled methyl end-group resonance for the epimerized diastereomer **II** over time. In practice, all aliquots provided ^{13}C NMR spectra with only a single ^{13}C -labeled methyl end-group for diastereomer **I**, even after 18 h of gestation. Accordingly, chain-end epimerization through enantiofacial switching does not appear to be possible for LPD, whereas chain-walking is. Finally, it must be mentioned that warming a sample of LPD, initially prepared at $-10\text{ }^\circ\text{C}$, to room temperature results in the nearly quantitative formation of a vinyl end-group through β -hydride elimination. Although studies are still underway to quantify the amount of saturated end-groups that might be produced through competitive cyclopentadienyl ligand H-abstraction, at the present it appears that this decomposition path does not compete with β -hydride elimination in LPD as effectively as it does in the model compounds **5e** and **5f**.

Since the *tert*-butyl derivative **5h** has not yet yielded to synthesis, it has not been possible to investigate the stability of this species relative to that of the isobutyl cation **5e**. However, with both the *n*-propyl and isopropyl derivatives, **5b** and **5c**, respectively, in hand, a similar investigation was conducted with them. As stated previously, both **5b** and **5c** remained unchanged over extended periods of time in chlorobenzene solution at $0\text{ }^\circ\text{C}$, a temperature at which both **5e** and **5f** undergo decomposition by β -hydride elimination and intramolecular H-abstraction. At $5\text{ }^\circ\text{C}$, however, the isopropyl complex **5c** was observed to isomerize fully to the *n*-propyl derivative **5b** in a first-order fashion (at $5\text{ }^\circ\text{C}$, $t_{1/2} = 68\text{ h}$; at $10\text{ }^\circ\text{C}$, $t_{1/2} = 33\text{ h}$), with only a trace amount of decomposition being observed. To determine if this isomerization process is reversible, decomposition of the deuterium-labeled *n*-propyl derivative **5b*** at more elevated temperatures was studied. Thus, at $20\text{ }^\circ\text{C}$, while **5b*** was observed to decompose in first-order fashion, the deuterium label in the β -position of the *n*-propyl substituent *did not scramble*, and this remained true at even higher temperatures of up to $50\text{ }^\circ\text{C}$. Interestingly, at no temperature was propene observed, and thus,

(36) (a) Schock, L. E.; Brock, C. P.; Marks, T. J. *Organometallics* **1987**, *6*, 232–241. (b) Bulls, A. R.; Schaefer, W. P.; Serfas, M.; Bercaw, J. E. *Organometallics* **1987**, *6*, 1219–1226. (c) Carney, M. J.; Walsh, P. J.; Bergman, R. G. *J. Am. Chem. Soc.* **1990**, *112*, 6426–6428. (d) Horton, A. D. *Organometallics* **1992**, *11*, 3271–3275. (e) Sun, Y.; Spence, R. E. v. H.; Piers, W. E.; Parvez, M.; Yap, G. P. A. *J. Am. Chem. Soc.* **1997**, *119*, 5132–5143.

Scheme 14



7

it is possible that intramolecular H-abstraction from the cyclopentadienyl ligand is now the dominant decomposition path for **5b**.

(g) Decomposition and Isomerization of Hafnium Derivatives. Upon quantitative generation through protonolysis, the cationic *tert*-butyl hafnium complex **7** was found to be unstable, isomerizing to the unlabeled isobutyl derivative of **6** at temperatures as low as $-35\text{ }^{\circ}\text{C}$. At $-10\text{ }^{\circ}\text{C}$, quantitative isomerization of **7** to **6** according to Scheme 14 was complete within 1 h, and through an Eyring analysis (five temperatures between -35 and $0\text{ }^{\circ}\text{C}$), the activation parameters for this process were determined to be $\Delta H^{\ddagger} = 16.4 \pm 0.5\text{ kcal mol}^{-1}$ and $\Delta S^{\ddagger} = -3.0 \pm 1.0\text{ eu}$.

Regarding decomposition of the unlabeled isobutyl derivative of **6**, relative to the zirconium analogue **5e**, the former compound was surprisingly found to be more unstable than the latter, and in fact, it slowly decomposes even at $-35\text{ }^{\circ}\text{C}$. Once again, the metal-containing product of decomposition is the dichloro dicationic species, $\{(\eta^5\text{-C}_5\text{Me}_5)\text{Hf}(\mu\text{-Cl})[\text{N}(\text{Et})\text{C}(\text{Me})\text{N}(\text{t-Bu})]\}_2[\text{B}(\text{C}_6\text{F}_5)_4]_2$, as previously reported.^{6h} At $0\text{ }^{\circ}\text{C}$, the rate of decomposition of **6** was measured to be 0.055 h^{-1} ($t_{1/2} = 12.6\text{ h}$), which can be compared to 0.034 h^{-1} ($t_{1/2} = 20.4\text{ h}$) for **5e** (vide supra). More interestingly, the β -hydrogen resonance for unlabeled **6** appears as a well-defined multiplet at 1.55 ppm. Thus, unlike the isobutyl zirconium complex **5e**, the hafnium analogue does not appear to possess a strong β -hydrogen agostic interaction in solution. Further, in contrast to the zirconium analogue **5e*****, the doubly labeled hafnium isobutyl derivative **6** did not show any evidence of isotopic label scrambling at $0\text{ }^{\circ}\text{C}$. Finally, analysis of the decomposition products at this temperature revealed that the quantities of 2-methylpropene and 2-methylpropane obtained were similar to those of the decomposition products of **5e*****, and accordingly, it appears that intramolecular H-abstraction from the cyclopentadienyl ligand in the isobutyl hafnium compound **6** is a competitive decomposition path, as it is for the zirconium series.

Discussion

The results obtained regarding the modes of decomposition for the cationic zirconium and hafnium alkyl complexes **5–7** allow us to perhaps paint a clearer picture of the steric and electronic factors that are important for establishing the living character of Ziegler–Natta polymerizations based on the class of initiators encompassed by **2**. This new insight will undoubtedly aid in efforts to design the next generation of initiators that are capable of operating at much higher temperatures. At the same time, however, when compared with results obtained from direct observation of the living polymeryl species themselves, distinct limitations have also been exposed regarding the ability of the “model” compounds to actually serve as reliable models.

To begin, the present studies have served to uncover a competitive intramolecular decomposition pathway that most

likely proceeds through H-abstraction from a methyl group of the cyclopentadienyl ligand of **5** to liberate an alkane. We do not yet know, however, how the steric and electronic factors of the alkyl/polymeryl substituent in the cationic zirconium complexes may either act in concert to promote this path as the dominant mode of decomposition in some cases or, alternatively, render it noncompetitive with β -hydride elimination in others. For instance, with living polymeryl species derived from the polymerization of higher α -olefins with **2a**, intramolecular H-abstraction from the cyclopentadienyl ligand does not appear to be as competitive with β -hydride elimination, possibly as a result of steric inhibition by the bulky polymeryl chain and backbone substituents. On the other hand, as we have yet to observe ethene, propene, or 1-butene in the decomposition of **5a**, **5b**, and **5d**, it is possible that, for these linear *n*-alkane substituents, intramolecular H-abstraction is now the dominant, if not single, mode of decomposition. We are presently engaged in the synthesis of **5** and living polymeryl species from **2a** in which deuterium labeling in the cyclopentadienyl methyl groups should allow us both to unequivocally establish this mode of decomposition and to quantify to what extent it occurs for the living polymeryl species at higher temperatures.

Given the uncertainty that still exists regarding the nature and extent to which the competitive H-abstraction reaction is contributing to the decomposition of **5**, quantitative kinetic analyses of β -hydride elimination for the different derivatives are not yet possible. However, general trends have been revealed by the present studies, and they suggest the relative importance of different steric and electronic effects on this process within living polymerizations initiated by **2a**. Perhaps of most surprising note was documentation of the relative stability of **5e** > **5f** > LPD at $0\text{ }^{\circ}\text{C}$. All three species possess a similarly configured β -substituted primary alkyl substituent, and therefore, from an electronic perspective, they would all appear rather similar. The observed decrease in stability on going from **5e** to **5f** to LPD, however, does track with an increase in the size of both this β -substituent and the entire alkyl substituent itself. There are two possible ways in which a steric factor can play a key role in determining stability within the series. First is the more obvious fact that, after initial β -hydride elimination, an increase in nonbonded interactions between the metal–ligand sphere and the newly generated alkene fragment should promote irreversible chain release of the latter. More problematic is the apparent result that, while **5e** and **5f** can engage in a strong β -hydrogen agostic interaction in solution, LPD cannot due to a similar increase in nonbonded interactions between the polymeryl substituent and the ligand sphere. At first glance, the association of a strong β -hydrogen agostic interaction with an increase in stability toward β -hydride elimination would appear contradictory. However, as first proposed by Bercaw and co-workers,³⁷ the ability to form a β -hydrogen agostic interaction with the highly electrophilic metal center might actually provide for ground-state stabilization. A significant barrier to β -hydride elimination would then still be in keeping with a late transition state in which substantial positive charge has developed on the β -carbon.^{12c,37} Observation that LPB can engage in chain-walking at $-10\text{ }^{\circ}\text{C}$, a temperature at which **5e***** does not engage in isotopic label scrambling, further supports a lower

(37) Burger, B. J.; Thompson, M. E.; Cotter, W. D.; Bercaw, J. E. *J. Am. Chem. Soc.* **1990**, *112*, 1566–1577.

barrier to β -hydride elimination for the living polymeryl species relative to that for the isobutyl model complex. It must be borne in mind, however, that the exact mechanism by which these structural isomerizations occur is still not well understood, and rather than proceeding through discrete alkene hydride intermediates arising from β -hydride elimination, it is possible that "metal-assisted" 1,2-hydride shifts are involved that occur in concerted fashion similar to that observed for other metal-assisted 1,*n*-hydride shifts and metal-assisted β -hydride transfer to monomer mechanisms that are supported by recent theoretical studies.^{14b,c,38} If so, the polymeryl species may actually be able to access the transition state for one of these 1,2-hydride shifts more readily in the absence of a strong β -hydrogen agostic interaction.

Regarding the relative stabilities of the *n*-propyl and isopropyl derivatives, **5b** and **5c**, respectively, it is not surprising that the linear primary *n*-alkyl substituent is favored over the secondary one.^{39,40} Although not yet quantified, it would also appear that a lower barrier to β -hydride elimination is present in **5e** and **5f** than in either **5b** or **5c**, even in the presence of strong β -hydrogen agostic interactions in all four. This observation is in keeping with a greater stabilization of a transition state with substantial positive charge on the β -carbon that is provided by the β -alkyl group on the alkyl substituent in the former pair.³⁷ It also seems quite reasonable that, after β -hydride elimination in **5e**, strong nonbonded interactions between the 2-methylpropene (isobutylene) fragment and the ligand sphere within an alkene hydride complex promote chain-release, leading to decomposition, whereas with **5c**, these steric interactions are greatly reduced with the coordinated propene within the alkene hydride, thus providing for greater stability through reinsertion, if indeed the **5c** \rightarrow **5b** isomerization does proceed through formal β -hydride elimination. A more seemingly inexplicable discovery is that, while the *n*-propyl derivative **5b** apparently does not (cannot) isomerize to the secondary isopropyl derivative **5c**, even at temperatures as high as 50 °C, the isobutyl derivative **5e** can undergo facile isomerization at the low temperature of 0 °C that presumably goes through intermediacy of what one would imagine to be the more sterically encumbered *tert*-butyl complex **5h**. In this regard, it is highly unfortunate that **5h** has not yet yielded to synthesis, as a crystal structure of this species should be highly informative regarding the steric and electronic factors that may serve to render this tertiary alkyl species more accessible from **5e** than the isopropyl complex **5c** is from **5b**. In fact, theoretical calculations predict that such a cationic zirconium tertiary alkyl complex actually possesses substantial positive charge on the tertiary carbon center that is stabilized by the three alkyl substituents.¹⁸

Of final note and importance is the observation that, in contrast to the results obtained by Schrock and co-workers, the isobutyl hafnium analogue of **5e** is less stable than its zirconium

cousin. One possible explanation for why the hafnium species does not appear to engage in a strong β -hydrogen agostic interaction in solution, while **5e** does, might be found in the observation that bond lengths between ligand fragments and the metal center within neutral dialkyl hafnium analogues of **4** are significantly shorter than in the zirconium counterparts, presumably due to the effects of lanthanide contraction.^{6h} Thus, for the unlabeled isobutyl derivative **6**, an increase in steric interactions may preclude formation of a ground-state stabilizing β -hydrogen interaction, and solid-state structural studies are continuing with the aim of either substantiating or disproving this conjecture. Finally, it is interesting to note that the isobutyl hafnium derivative **6** does not engage in isotopic label scrambling through structural isomerizations that formally involve the *tert*-butyl derivative **7**, and that this former species is clearly more thermodynamically favored over the latter, which can undergo isomerization with a modest barrier.

Conclusions

For as much success as has recently been reported regarding the development of early transition metal-based initiators that can effect the living Ziegler–Natta polymerization of ethene, propene, and higher α -olefins, general knowledge of the steric and electronic factors that contribute to rendering these systems living is still lacking. The present extensive study of different structural model complexes for the living system based on **2a** has served to delineate the extent to which these complexes are actually useful for realistically modeling the living polymeryl species. At one extreme, there is clear evidence to suggest that new modes of decomposition, such as the postulated intramolecular H-abstraction process, might be more relevant to only the model complexes. On the other hand, the model complexes have served to reveal some general trends that should prove useful in either designing new initiators for high-temperature living polymerization or making predictions regarding which systems should be more intrinsically stable. With respect to this latter point, results obtained with the linear primary alkane model complexes suggest that these species are intrinsically more stable toward β -hydride elimination than those possessing β -alkyl substituents. When translated to practice, this conclusion then supports the prediction that the living polymerization of ethene by the class of initiators represented by **2** should be amenable to much higher temperatures than the living polymerization of either propene or higher α -olefins. Efforts to substantiate this prediction are currently in progress.

Acknowledgment. Funding for this work was provided by the NSF (CHE-0092493), for which we are grateful. We also thank the ACS Division of Organic Chemistry for graduate fellowships to both M.B.H. and R.J.K., sponsored by the Proctor and Gamble Co.

Supporting Information Available: Experimental details, including ¹H NMR, of compounds **5a–d,f**, **5b***, **5e***, **5e****, **5e*****, **6**, and **7**, and details of crystallographic analyses of compounds **3c,e–g**, **4a,c–e**, **5e**, and **14** (PDF, CIF). This material is available free of charge via the Internet at <http://pubs.acs.org>.

JA057866V

(38) Yu, Z.-X.; Houk, K. N. *Angew. Chem., Int. Ed.* **2003**, *42*, 808–811.

(39) Coleman, J. P.; Hedgedus, L. S.; Norton, J. R.; Finke, R. G. *Principles and Applications of Organotransition Metal Chemistry*; University Science: Mill Valley, CA, 1987.

(40) It is interesting to note that the reverse trend appears true within model complexes for the late transition metal living polymerization system studied by Brookhart and co-workers, see: (a) Shultz, L. H.; Tempel, D. J.; Brookhart, M. *J. Am. Chem. Soc.* **2001**, *123*, 11539–11555. (b) Leatherman, M. D.; Svejda, S. A.; Johnson, L. K.; Brookhart, M. *J. Am. Chem. Soc.* **2003**, *125*, 3068–3081.